

# Supplementary Information for “Boundary layer water vapour statistics from high-spatial-resolution spaceborne imaging spectroscopy”

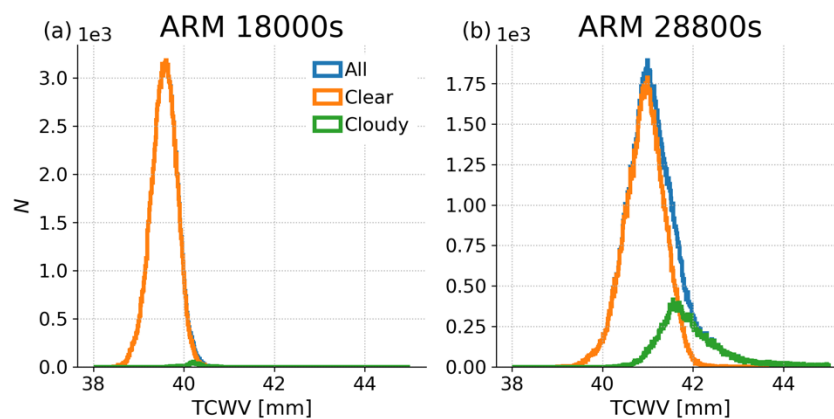
Mark Richardson<sup>1,2</sup>, David R. Thompson<sup>1</sup>, Marcin Kurowski<sup>1</sup>, Matthew D. Lebsock<sup>1</sup>

5 <sup>1</sup>Jet Propulsion Laboratory, California Institute of Technology, Pasadena, CA 91109, USA

<sup>2</sup> Department of Atmospheric Science, Colorado State University, Fort Collins, CO 90095, USA

Correspondence to: Mark Richardson ([markr@jpl.nasa.gov](mailto:markr@jpl.nasa.gov))

## 1 Clear- versus all-sky statistics



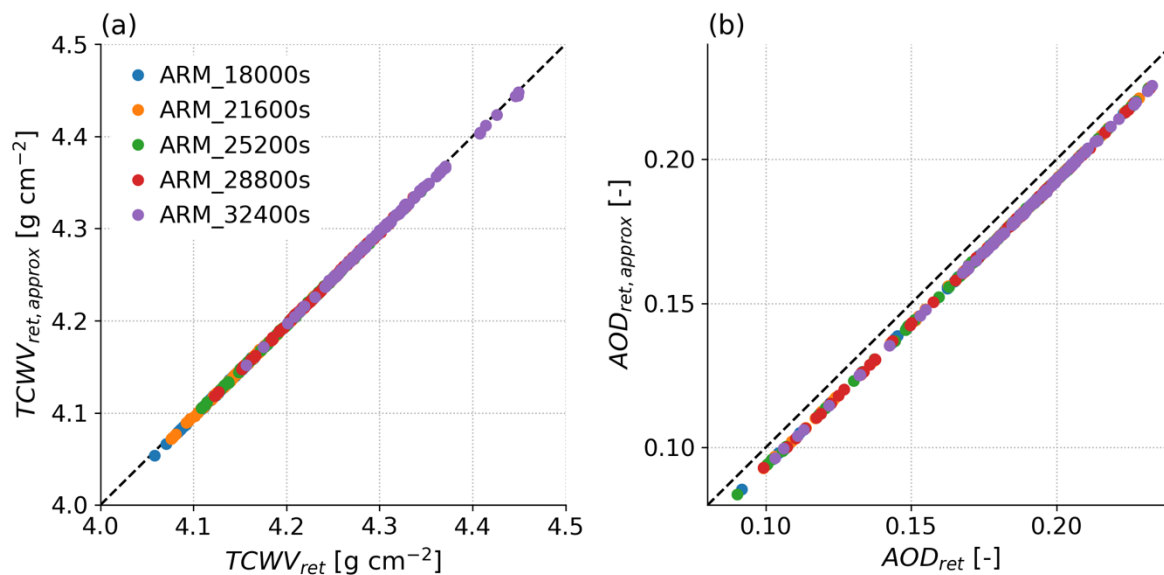
10

**Supplementary Figure 1. Histograms of TCWV for all columns in (a) the 18000 second snapshot of the ARM LES and (b) the 28800 s snapshot of the same. The blue histograms show all columns, the orange histograms the clear-sky only (defined as estimated  $\tau_{\text{cloud}} < 0.3$ ) and the green the cloudy-sky footprints. Cloud fraction increases from 0.7 % to 21.1 % between the snapshots.**

15

20

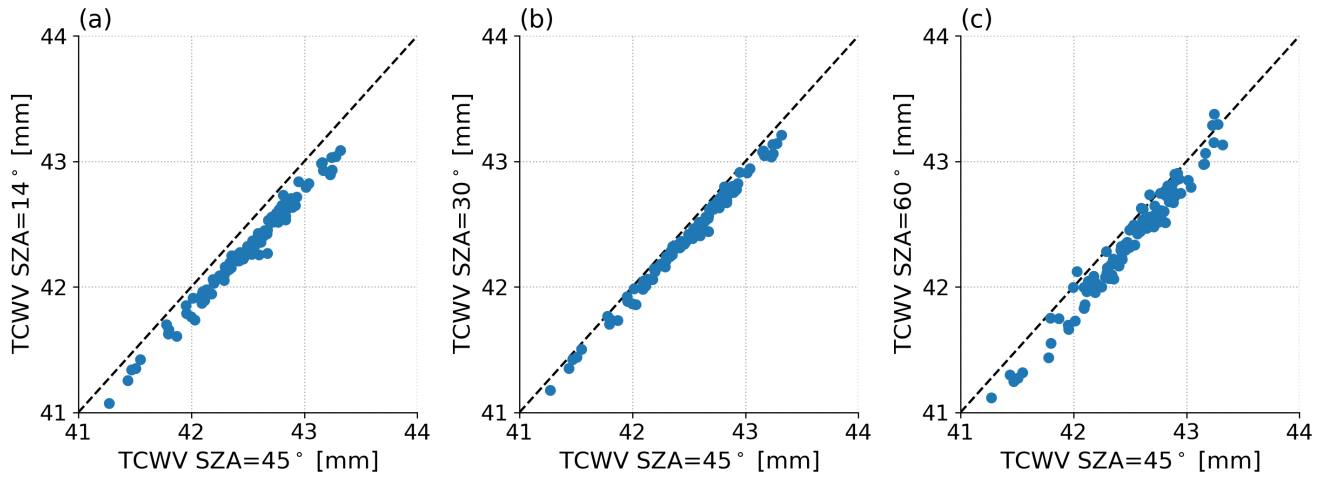
## 2 Use of simplified forward model in retrieval



Supplementary Figure 2. (a) retrieved TCWV and (b) retrieved AOD when using the forward model approximation as a function of the same retrieved values when providing MODTRAN with the surface  $\rho_s$  spectrum as input. For the same  $N=101$  footprints as in the main paper and a subset of ARM snapshots.

### 3 Solar zenith angle tests

The 101 footprints from ARM\_18000s were simulated and retrieved as in the main manuscript but for SZAs of 14°, 30°, 45° and 60°, each with its own lookup table. The forward model was the simplified Lambertian Eq. (1) with a MODTRAN cropland surface underneath, and the lookup table used the midlatitude summer atmosphere. Supplementary Figure 3 shows how each of the other SZA retrievals relates to those at SZA=45°. More scatter is visible at SZA=60°, and the statistics of the snapshot and the biases and standard deviations of differences relative to the truth are listed in **Error! Reference source not found.** The biases and standard deviations both vary significantly at  $2\sigma$ .



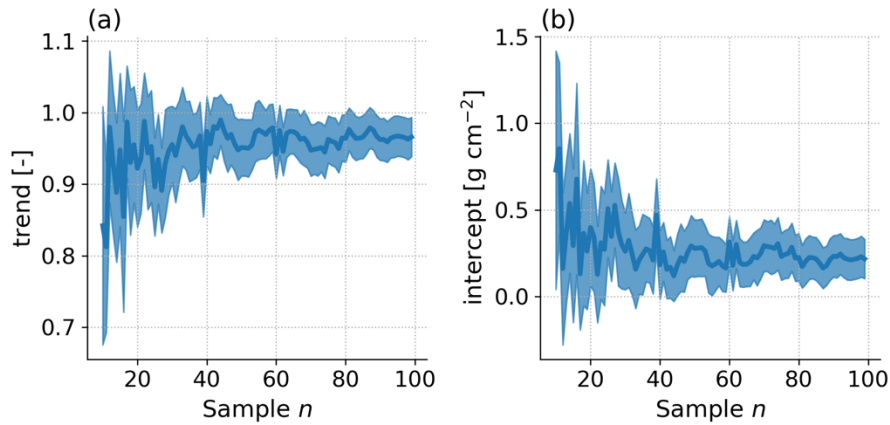
Supplementary Figure 3. Retrieved TCWV for the ARM\_18000s snapshot as SZA varies, plotted as a function of the retrieved value at SZA=45°. (a) SZA=14°, (b) SZA=30°, (c) SZA=60°

15

20

#### 4 Sample size and emulator fits

The main manuscript emulators used 303—707 data points, with 101 from each snapshot in the relevant case. It was not known *a priori* that the snapshots could be combined, so we required a sample size that would produce stable emulator parameters from a single snapshot. This was confirmed by incrementally increasing sample size and fitting emulator parameters until the parameters stabilised such that a larger sample size did not change the results. This is confirmed for ARM\_18000s in Supplementary Figure 4, where parameters stabilise below  $N=101$ . These results are characteristic of other snapshots (not shown).



Supplementary Figure 4. (a) slope and (b) intercept parameters from linear fits between TCWV and TCWV<sub>ret</sub> in ARM\_18000s for random subsamples of footprints with increasing sample size.

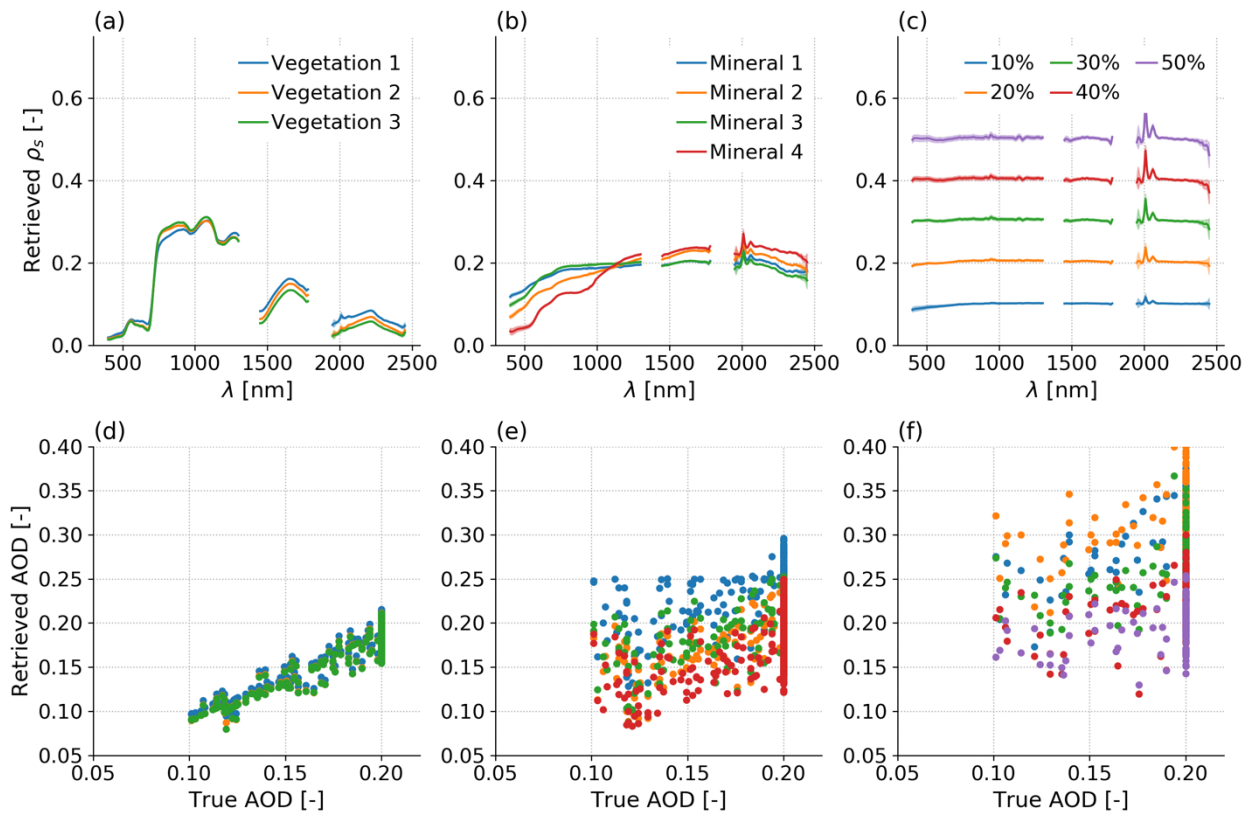
15

20

## 5 Aerosol optical depth and water vapour retrieval co-dependence

A coding error assigned AOD=0.2 to most footprints rather than evenly sampling from AOD of 0.1–0.2. Supplementary Figure 5 shows that the AOD retrieval performs well over vegetated surfaces, but that darker and flatter surface  $\rho_s$  spectra degrade the correlation, bias and spread. Comparing panels (e,f) with their associated surfaces (b,c), the retrieval generally compensates for darker surfaces by increasing the AOD. This larger simulated AOD likely explains the  $\lambda < 800$  nm curvature in the retrieved  $\rho_s$  for the 10 % and 20 % Lambertian surfaces. Additionally, darker and flatter surface spectra are associated with a loss of correlation between AOD and AOD<sub>ret</sub>. This confirms unsurprising relationships between retrieved AOD and  $\rho_s$ , but the question of interest for this study is whether the relationship between TCWV and TCWV<sub>ret</sub> is strongly affected by AOD.

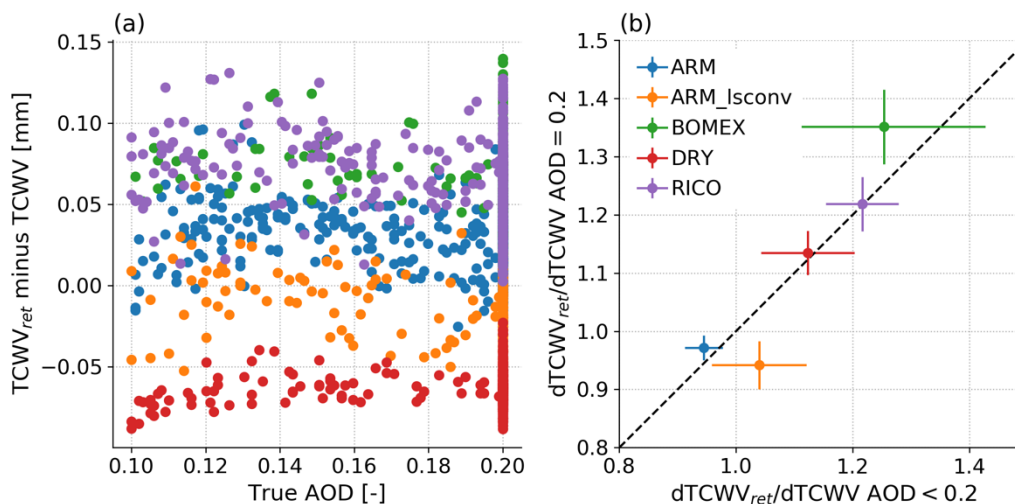
10



Supplementary Figure 5. As main text Figure 4 but (d–f) have been replaced with retrieved AOD as a function of true AOD.

15

Supplementary Figure 6 shows that the  $TCWV_{ret}$  bias differences between snapshots are far larger than any shift induced by background AOD, and also shows the emulator trend parameters calculated for each LES case when separately fitting to footprints with AOD=0.2 or AOD<0.2. There is a significant difference ( $p<0.05$ ) in ARM\_Isconv but no others. This is evidence that in some cases, changes in background AOD could affect derived spatial statistics, but once again, the differences induced by AOD are substantially smaller than those caused by different meteorological conditions or surface type. We also considered  $TCWV_{ret}$  minus  $TCWV$  as a function of  $AOD_{ret}$  minus  $AOD$ , but results were very similar to panel (a).



10 **Supplementary Figure 6. (a) Footprint  $TCWV_{ret}$  minus true  $TCWV$  as a function of true AOD (b) Slopes  $\pm 2\sigma$  error of  $TCWV_{ret}$  regressed against  $TCWV$  for the subset in each case with AOD=0.2 versus the subset with AOD<0.2. Differences are significant at  $2\sigma$  when the ellipse defined by the error bars is not intersected by the dashed 1:1 line. This is only true for ARM\_Isconv.**

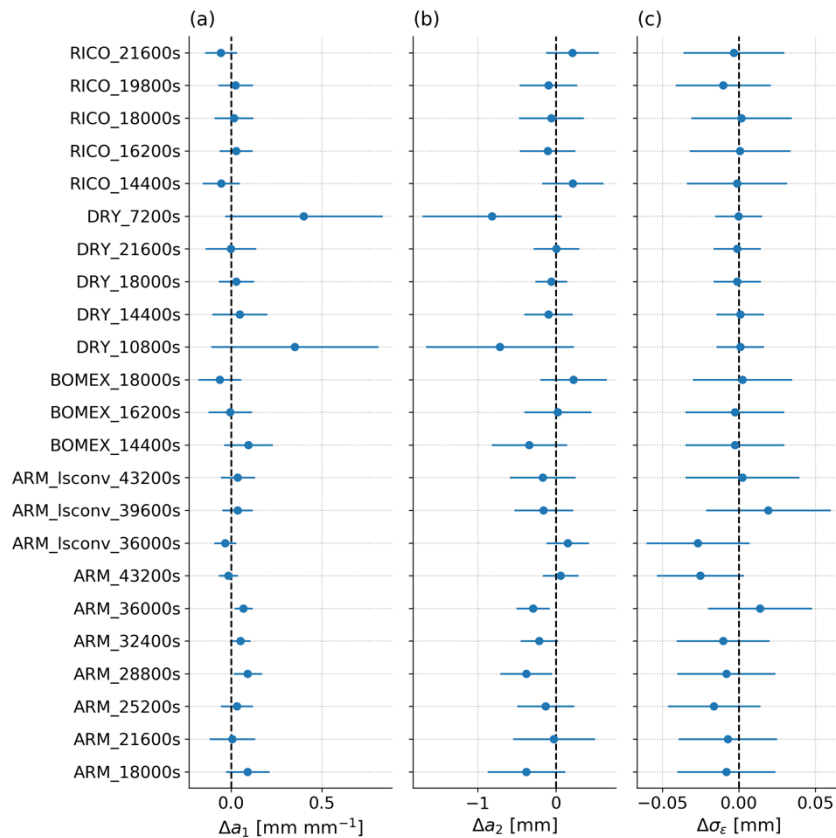
15

20

## 6 Emulators fit to individual snapshots versus all snapshots in a case

Emulators were fit to each of the individual snapshots and their best fit parameters compared with those obtained from fits to the full snapshot datasets. While individual snapshots will clearly differ somewhat, we question whether these differences are likely to be substantial and whether they can be detected with significance.

- 5 Of the 23 snapshots, Supplementary Figure 7 shows that 2 had significant ( $p < 0.05$ ) differences in  $a_1$  (slope) and  $a_2$  (intercept), and zero had differences in  $\sigma_\varepsilon$  (random error). From a sample of 23, the 95 % confidence interval of the number of samples that will be different at  $2\sigma$  is 0—4, so we do not have evidence of systematic differences between the emulators fit to individual snapshots versus individual cases. This contrasts with the differences between cases, where there are more significant differences. We note that some of the best-fit differences are substantial, particularly DRY\_7200s and DRY\_10800s, but this
- 10 is because they show small spread in TCWV and therefore large uncertainty in their estimated  $dTCWV_{ret}/dTCWV$ .



Supplementary Figure 7. Differences in emulator parameters for each snapshot relative to those calculated using all snapshots in each case. (a) slope parameter  $a_1$ , (b) intercept parameter  $a_2$ , (c) standard deviation of residuals  $\sigma_\varepsilon$ . In all cases the points are best estimates, the error bars are  $2\sigma$  and differences of zero are shown by vertical dashed lines.

15

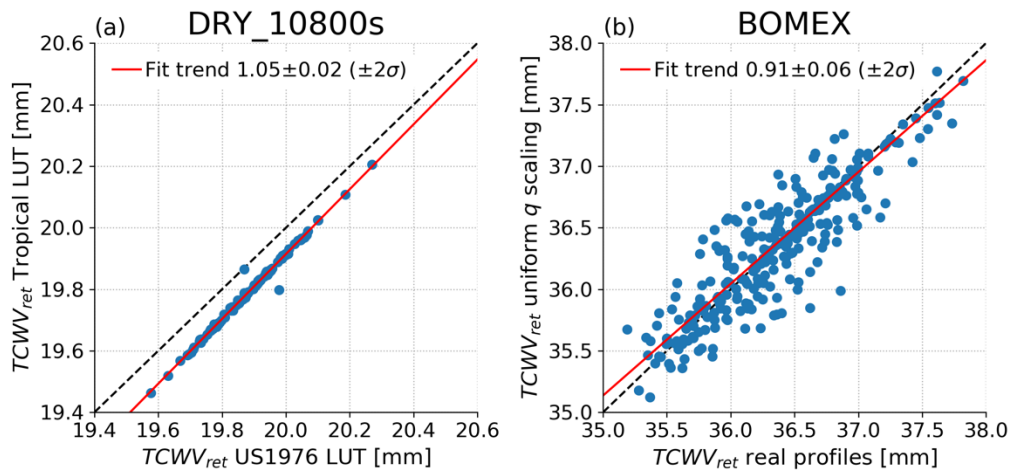
## 7 Atmospheric sensitivity tests

Results from two tests of how atmospheric conditions affect retrieval sensitivity are in Supplementary Figure 8. The panel (a) test needs just one snapshot since it uses one set of observations with identical error, meaning that scatter is very small and  $N=101$  is sufficient for calculation of statistics. A DRY snapshot is used since this allows application of the U.S. Standard Atmosphere 1976 LUT, whose maximum possible TCWV is higher than in DRY but lower than in the other cases.

In panel (a), using the warmer tropical atmosphere to develop the LUT means lower retrieved TCWV. This follows qualitative expectations from a simplified model: a warmer atmosphere means more line broadening such lower TCWV is needed to generate a given amount of absorption.

Of relevance for local spatial statistics, the regression slope shows 5 % higher sensitivity when using the tropical LUT rather than the U.S. Standard Atmosphere 1976 LUT. DOAS retrievals exploit how absorption is a logarithmic function of TCWV, such that sensitivity  $dI/dTCWV$  is nonlinear. The exact response of the retrieval will also depend on TCWV, channels used and the atmosphere, and test (a) demonstrates that this can affect retrieved statistics.

In panel (b) all BOMEX snapshots are used, and this was selected as BOMEX showed the largest  $dTCWV_{ret}/dTCWV$ . The larger sample size from all snapshots was needed since in this case the forward model radiances are changed, and the varying retrieval error between simulations of the same footprint results in greater scatter. This shows that when the forward model simply scales the median  $q(z)$  profile, that the sensitivity is 9 % lower than when the real profile variation is simulated. This change will likely change further with aerosol or temperature profile changes, but it appears that implementing a LUT approach where variability is constrained to lower altitudes might result in more realistic atmospheric retrievals.



Supplementary Figure 8. Comparison of pairs of TCWV retrievals, (a) in the DRY\_18000s snapshot, results when using the MODTRAN6.0 default tropical atmosphere in the LUT as a function of the results when using the U.S. Standard Atmosphere 1976, (b) for all BOMEX snapshots where each footprint uses the median  $q(z)$  profile that is uniformly scaled to match original TCWV, as a function of the default approach using the true LES profiles for each snapshot. Dashed black 1:1 lines are appended, and best fit slopes with  $\pm 2\sigma$  errors are labelled in the legend.

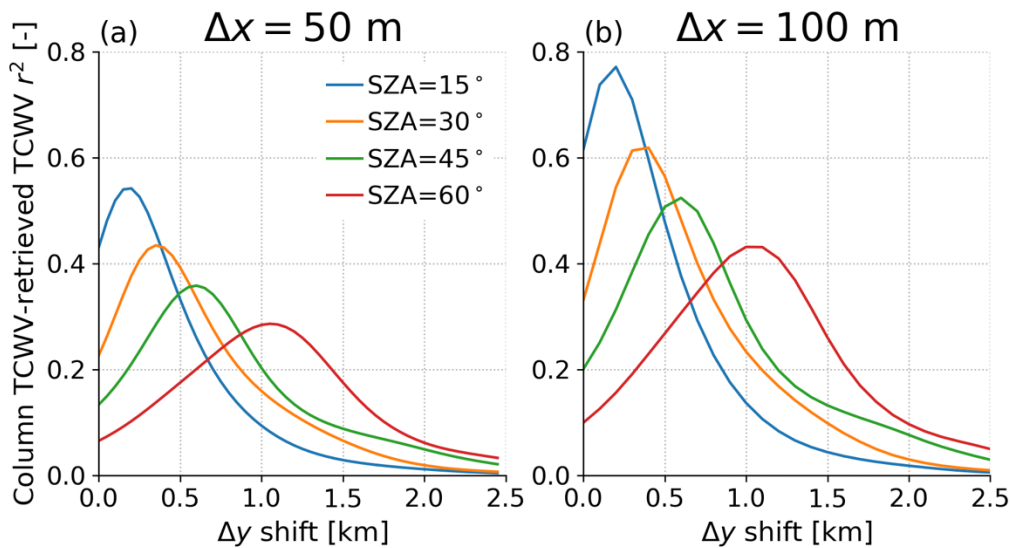


## 8 Shifting retrieved field to account for non-vertical solar path

The simulated sunlight follows a downward path at the SZA and a direct upward path. Clearly the downward path is longer due to its horizontal component, and therefore the overall path contains proportionally more downward path than upward path. The vertical profiles  $q(z)$  in Figure 1 show that each LES snapshot contains a characteristic layer, typically near the PBL top, at which the majority of TCWV variability occurs. It is therefore fair to ask whether the spatial pattern of  $\text{TCWV}_{\text{ret}}$  will correspond better to the spatial pattern of integrated  $q$  at the horizontal location corresponding to where the sunlight passes downward through that layer, as opposed to the TCWV evaluated at the nominal surface footprint.

To assess this, we translated the  $\text{TCWV}_{\text{ret}}$  field towards the incoming sunlight (along the positive  $y$  direction) and recalculated the  $r^2$  for translations from 0—2.5 km. Supplementary Figure 9 shows the results for the ARM\_18000s case at native resolution and after smoothing to  $\Delta x = 100$  m. There is indeed a peak in correlation coefficient corresponding to the location at which the  $\text{TCWV}_{\text{ret}}$  map lines up with the location at which the downward solar path passes through the layer of largest horizontal  $q$  variation. However, the performance is still substantially lower than for  $\text{SZA}=0^\circ$ . Results are similar for other snapshots, albeit the DRY cases show significantly worse performance.

15



Supplementary Figure 9. Calculated  $r^2$  between TCWV and  $\text{TCWV}_{\text{ret}}$  fields at ARM\_18000s as a function of horizontal spatial offset. The  $\text{TCWV}_{\text{ret}}$  field is shifted one footprint at a time in the positive the  $y$  direction and  $r^2$  is recalculated. Lines show different SZA as labelled in the legend of (a), which contains native resolution output while (b) shows the results when TCWV and  $\text{TCWV}_{\text{ret}}$  are first smoothed to 100 m resolution.

20